

# Journal of Mechanics of Materials and Structures

**SLIDING OF A CUP-SHAPED DIE ON A HALF-SPACE: INFLUENCE OF  
THERMAL RELAXATION, CONVECTION AND DIE TEMPERATURE**

Louis Milton Brock

**Volume 9, No. 3**

**May 2014**





## SLIDING OF A CUP-SHAPED DIE ON A HALF-SPACE: INFLUENCE OF THERMAL RELAXATION, CONVECTION AND DIE TEMPERATURE

LOUIS MILTON BROCK

A rigid, cup-shaped die translates at constant subcritical speed on a thermoelastic half-space that exhibits thermal relaxation and convection. The die surface is held at a temperature different from ambient temperature, and sliding friction exists in a contact zone that is not simply connected. A three-dimensional dynamic steady state model is assumed and, based on an approximation for inversion of integral transforms, a solution in analytic form is obtained. Auxiliary conditions for sliding contact are satisfied; in particular, contact zone traction is stationary with respect to compression force. Among other results, it is found that a dynamic steady state is precluded if die-ambient temperature difference is too large. Similar results are known, but only for die temperatures that exceed the ambient value.

### Introduction

Sliding of a rigid die on the surface of elastic half-spaces is a basic model in isothermal [Craggs and Roberts 1967; Churilov 1978; Ahmadi et al. 1983; Rahman 1996] and dynamic thermoelastic contact [Jang 2000; 2005]. In [Brock 2012a] the 3D problem of an ellipsoid moving at constant sub critical speed is considered. An exact solution for the dynamic steady state shows that the projection of the die profiles onto the half-space is not necessarily replicated in contact zone shape. In particular, friction and sliding speed play a role in contact zone shape. An asymptotic solution [Brock 2012b] is obtained for the corresponding 3D case of a half-space governed by the Fourier model of thermoelasticity [Boley and Weiner 1985]. Expressions in analytic form lead to conclusions about the contact zone that mirror those in [Brock 2012a].

A more recent 3D study [Brock 2014b] treats various die shapes. Friction is neglected, but the half-space exhibits both thermal relaxation and convection, and the dies are maintained at a fixed temperature. Again expressions in analytic form are obtained by using an asymptotic transform inversion. It is found that a dynamic steady state cannot in fact occur when die temperature exceeds ambient temperature by a critical value. This result is consistent with transient work [Jang 2000; 2005].

In the aforementioned references, however, the die shapes considered give simply connected contact zones. Such a situation is not always assured [Bayer 1994; Blau 1996]. Die surfaces may exhibit curvature reversals that preclude simple connectivity and, as an example, this paper considers a cup-shaped rigid die. The half-space exhibits thermal relaxation and convection, and the die surface is maintained at a fixed temperature that differs from the ambient. A dynamic steady state is assumed, and sliding friction exists. A contact zone traction distribution is not assumed and contact zone geometry parameters are obtained by imposing standard [Barber 1992; Brock and Georgiadis 2000] auxiliary conditions. Here,

---

*Keywords:* thermoelasticity, 3D, relaxation, multiple connectivity, critical temperature, convection, 3D dynamic, sliding, transverse isotropy, contact zone geometry.

these conditions lead to algebraic equations of fifth- and sixth-order, but valid approximate solutions are possible. Among other results, this analysis indicates that, in contrast to [Jang 2000; 2005; Brock 2014b] restrictions apply for die temperature values both above and below ambient temperature.

The 3D analysis begins by considering the unmixed boundary value problem for surface loads applied to an area that translates on the half-space surface. The area is ring-like, but axial symmetry is not assumed. An exact solution for the integral transform is obtained in terms of (somewhat arbitrary) loads. An approximate transform inversion technique that is especially valid when thermal relaxation effects are of interest is applied. The resulting expressions are analytic, and their use reduces the mixed boundary value problem for sliding contact to the solution of classical singular integral equations [Erdogan 1978]. Imposition of auxiliary conditions, and study of the results, follows.

### Translating surface load: governing equations

In terms of Cartesian basis  $\mathbf{x} = \mathbf{x}(x_k)$  a solid occupies region  $x_3 > 0$ . The solid is isotropic, homogeneous and linear thermoelastic. It is at rest at uniform (absolute) temperature  $T_0$ , when a finite, ring-like area  $C$  on surface  $x_3 = 0$  is subjected to traction and a temperature field  $T_C \neq T_0$ . Curves  $f(x_1, x_2) = 0$  and  $\mathfrak{S}(x_1, x_2) = 0$  define, respectively, the inner and outer boundaries of  $C$ . Neither curve is necessarily circular, but is closed, with a tangent and normal that vary continuously. Each radius of curvature also varies continuously, without inflection. Surface point  $(x_1, x_2) = 0$  lies within contour  $f$ , and any straight line through this point lies within contour  $\mathfrak{S}$ .

Area  $C$  then translates in the positive  $x_1$ -direction with constant subcritical speed  $V$ . The geometry of  $C$  does not change, and imposed temperature  $T_C$  and the traction distribution remain invariant with respect to  $C$ . It is assumed that a dynamic steady state ensues for which solid response is invariant in the frame of translating  $C$ . Thus, by translating the Cartesian basis with  $C$ , displacement  $\mathbf{u}(u_k)$ , traction  $\mathbf{T}(\sigma_{ik})$  and change  $\theta$  in temperature vary only with  $\mathbf{x}(x_k)$ , and time differentiation becomes  $-V\partial_1$ , where  $\partial_k$  signifies  $x_k$ -differentiation. For  $x_3 > 0$  governing equations for  $(\mathbf{u}, \theta)$  can be written as [Brock 2009; Ignaczak and Ostoja-Starzewski 2010]

$$\mathbf{u} = \mathbf{u}_D + \mathbf{u}_S, \quad (1a)$$

$$(\nabla^2 - c^2\partial_1^2)\mathbf{u}_S = 0, \quad \nabla \cdot \mathbf{u}_S = 0, \quad (1b)$$

$$(c_D^2\nabla^2 - c^2\partial_1^2)\mathbf{u}_D - \alpha_V\nabla\theta = 0, \quad \nabla \times \mathbf{u}_D = 0, \quad (1c)$$

$$[h_0(c_+^2\nabla^2 - c^2\partial_1^2)(c_-^2\nabla^2 - c^2\partial_1^2) - c\partial_1(c_F^2\nabla^2 - c^2\partial_1^2)](\mathbf{u}_D, \theta) = 0. \quad (1d)$$

Here  $(\nabla, \nabla^2)$  are the gradient and Laplacian. Traction  $\mathbf{T}$  is defined by

$$\frac{1}{\mu}\mathbf{T} = [(c_D^2 - 2)\nabla \cdot \mathbf{u}_D - \alpha_V\theta]\mathbf{1} + 2(\nabla\mathbf{u} + \mathbf{u}\nabla). \quad (2)$$

Term  $\mathbf{1}$  is the identity tensor, and  $(c, c_D, c_F, c_{\pm})$  are dimensionless ratios

$$c = \frac{V}{V_S}, \quad c_D = \frac{V_D}{V_S}, \quad c_F = \frac{V_F}{V_S}, \quad c_{\pm} = \frac{V_{\pm}}{V_S}. \quad (3)$$

Here  $(V, V_S, V_D, V_F, V_{\pm})$  are, respectively, translation speed, isothermal shear wave speed, isothermal and Fourier dilatational wave speed and thermal relaxation speeds, where

$$c_D = \sqrt{2 \frac{1-\nu}{1-2\nu}}, \quad c_F = \sqrt{c_D^2 + \epsilon}, \quad c_{\pm} = \frac{1}{2}(\Gamma_+ \pm \Gamma_-), \quad (4a)$$

$$\Gamma_{\pm} = \sqrt{(c_D \pm \sqrt{h/h_0})^2 + \epsilon}, \quad (4b)$$

$$h = \frac{k}{C_V \sqrt{\mu\rho}}, \quad h_0 = V_S t_0, \quad \epsilon = \frac{T_0}{C_V} (\alpha_V V_S), \quad (4c)$$

$$\alpha_V = (3c_D^2 - 4)\alpha, \quad V_S = \sqrt{\mu/\rho}. \quad (4d)$$

In (2)–(4) ( $\nu$ ,  $\mu$ ,  $\rho$ ) are Poisson's ratio, shear modulus and mass density, respectively. Terms ( $k$ ,  $C_V$ ,  $\alpha$ ,  $\alpha_V$ ) are thermal conductivity, specific heat at constant strain, and linear and volumetric thermal expansion coefficients, respectively. Terms ( $\epsilon$ ,  $h$ ) are dimensionless thermal coupling constant and thermoelastic characteristic length. Terms ( $t_0$ ,  $h_0$ ) are thermal relaxation time and corresponding characteristic length [Brock 2009]. They are features of the Lord and Shulman [1967] model for thermal relaxation that is incorporated in (1)–(4). Calculations [Achenbach 1973; Brock and Georgiadis 2000; Brock 2009; Ignaczak and Ostoja-Starzewski 2010] indicate that, in general,  $1 < c_D < c_F < c_{\pm}$ .

On surface  $x_3 = 0$  heat flux and surface traction for  $(x_1, x_2) \notin C$  are

$$h_B \partial_3 \theta + \theta = 0, \quad \sigma_{31} = \sigma_{32} = \sigma_{33} = 0. \quad (5a)$$

For  $(x_1, x_2) \in C$ , however:

$$h_B \partial_3 \theta + \theta = T_C - T_0 = \theta_C, \quad (5b)$$

$$\sigma_{31} = \tau_1, \quad \sigma_{32} = \tau_2, \quad \sigma_{33} = \sigma. \quad (5c)$$

Field  $T_C$  is bounded and continuous, and  $h_B$  is a characteristic convection length that incorporates conductivity and Biot number [Boley and Weiner 1985]. Traction ( $\tau_1$ ,  $\tau_2$ ,  $\sigma$ ) can be singular but integrable on contours  $f(x_1, x_2) = 0$  and  $\mathfrak{S}(x_1, x_2) = 0$ . In addition  $(\mathbf{u}, \mathbf{T}, \theta)$  should remain finite for  $|\mathbf{x}| \rightarrow \infty$ ,  $x_3 > 0$ .

### General transform solution

A double bilateral transform [Sneddon 1972] can be defined as

$$\hat{F} = \iint F(x_1, x_2) \exp(-p_1 x_1 - p_2 x_2) dx_1 dx_2. \quad (6)$$

Integration is along the entire  $\text{Re}(x_1)$  and  $\text{Re}(x_2)$ -axes. Application of (6) to (1) gives

$$\hat{\mathbf{u}}_S = \mathbf{V} \exp(-B x_3), \quad (7a)$$

$$\hat{\mathbf{u}}_D = \mathbf{U}_+ \exp(-A_+ x_3) + \mathbf{U}_- \exp(-A_- x_3), \quad (7b)$$

$$\hat{\theta} = D_+ U_+ \exp(-A_+ x_3) + D_- U_- \exp(-A_- x_3). \quad (7c)$$

Coefficients  $D_{\pm}$  and the components of vectors  $(\mathbf{V}, \mathbf{U}_{\pm})$  are governed by

$$D_{\pm} = c_D^2 (p_2^2 + A_{\pm}^2) + (c_D^2 - c^2) p_1^2, \quad (8a)$$

$$p_1 V_1 + p_2 V_2 - B V_3 = 0, \quad \mathbf{U}_{\pm} = (p_1, p_2, -A_{\pm}) \alpha_V \mathbf{U}_{\pm}. \quad (8b)$$

Terms  $(B, A_{\pm})$  are roots of the transforms of, respectively, (1b) and (1d):

$$B = \sqrt{-p_1^2 - p_2^2 + c^2 p_1^2}, \quad (9a)$$

$$A_{\pm} = \sqrt{-p_1^2 - p_2^2 - \frac{cp_1}{2hc_D^2}(D_F \pm D)}, \quad (9b)$$

$$D_F = c_F^2(1 - h_0cp_1) - hcp_1, \quad D = \sqrt{D_F^2 + 4hc_D^2(1 - h_0cp_1)cp_1}. \quad (9c)$$

Equation (7) is bounded for  $x_3 > 0$  if branch cuts are introduced so that  $\text{Re}(B, A_{\pm}) \geq 0$  in the cut complex  $(p_1, p_2)$ -planes. Application of (6) to (2) and substitution of (8) and (9) gives for  $x_3 = 0$  quantities relevant to the transform of (5). In particular,

$$\frac{1}{\mu} \hat{\sigma}_{31} = -2\alpha_V p_1(A_+U_+ + A_-U_-) + \frac{1}{B}[p_1p_2V_2 + (p_1^2 - B^2)V_1], \quad (10a)$$

$$\frac{1}{\mu} \hat{\sigma}_{32} = -2\alpha_V p_2(A_+U_+ + A_-U_-) + \frac{1}{B}[p_2p_1V_1 + (p_2^2 - B^2)V_2], \quad (10b)$$

$$\frac{1}{\mu} \hat{\sigma}_{33} = -\alpha_V(2B^2 + c^2p_1^2)(U_+ + U_-) - 2(p_1V_1 + p_2V_2). \quad (10c)$$

In view of (7c) and (9), the transform of (5) gives the four equations required to obtain  $(U_{\pm}, V_1, V_2)$ . The transforms  $(\hat{\mathbf{u}}, \hat{\mathbf{T}}, \hat{\theta})$  then follow as linear combinations of  $(\hat{\tau}_1, \hat{\tau}_2, \hat{\sigma}, \hat{\theta}_C)$ . Displacement  $\mathbf{u}$  for  $x_3 = 0$  is required to address the mixed boundary value problem of the sliding die.

### Transform inversion: general formulas

Inhomogeneous terms  $(\tau_1, \tau_2, \sigma, \theta_C)$  arise only for  $(x_1, x_2) \in C$ . Thus, when  $x_3 = 0$  the inversion operation corresponding to (6) gives  $\mathbf{u}$ , and also  $(T, \theta)$ , as linear combinations of expressions

$$\iint_C \Sigma d\xi_1 d\xi_2 \frac{1}{2\pi i} \int dp_1 \frac{1}{2\pi i} \int K_{\Sigma} dp_2 \exp[p_1(x_1 - \xi_1) + p_2(x_2 - \xi_2)]. \quad (11)$$

Here  $\Sigma = \Sigma(\xi_1, \xi_2)$  represents  $(\tau_1, \tau_2, \sigma, \theta_C)$  and  $K_{\Sigma} = K_{\Sigma}(p_1, p_2)$  is the corresponding coefficient. Subscript  $C$  signifies integration over area  $C$ , and single integration is over the entire  $\text{Im}(p_1)$  and  $\text{Im}(p_2)$ -axes. The form of (11) suggests definitions and transformations [Brock 2012a; 2012b].

$$p_1 = p \cos \psi, \quad p_2 = p \sin \psi, \quad (12a)$$

$$\begin{bmatrix} x, \xi \\ y, \eta \end{bmatrix} = \begin{bmatrix} \cos \psi & \sin \psi \\ -\sin \psi & \cos \psi \end{bmatrix} \begin{bmatrix} x_1, \xi_1 \\ x_2, \xi_2 \end{bmatrix}. \quad (12b)$$

In (12),  $\text{Re}(p) = 0+$ ,  $|\text{Im}(p)|, x, y, \xi, \eta| < \infty$  and  $|\psi| < \pi/2$ . Parameters  $(p, \psi), (x, \psi; y = 0)$  and  $(\xi, \psi; \eta = 0)$  resemble quasipolar coordinate systems, i.e.,

$$d\xi_1 d\xi_2 = |\xi| d\xi d\psi, \quad dp_1 dp_2 = |p| dp d\psi. \quad (13)$$

In light of (12), (13) and conditions for contour functions  $(f, \mathfrak{S})$ , (11) can be written as

$$\frac{1}{i\pi} \int_{\Psi} d\psi \iint_C d\eta d\xi \Sigma(\xi, \eta) \int \frac{|p| dp}{2\pi i} K_{\Sigma}(p, \psi) \exp(p(x - \xi)). \quad (14a)$$



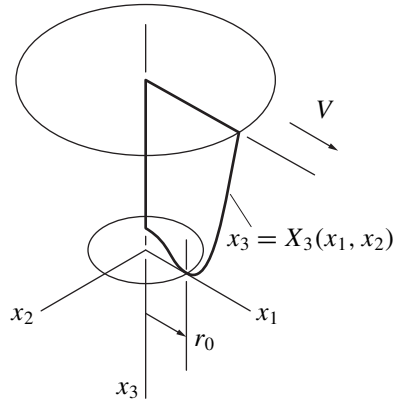


**Figure 1.** Schematic of area of revolution for sliding cup.

Here subscript  $\Psi$  signifies integration over range  $|\psi| < \pi/2$ ,  $p$ -integration is along the positive side of the entire imaginary axis, and

$$\iint_{\pm} d\eta d\xi = \left[ \int_{N^-}^{\eta^-} + \int_{\eta^+}^{N^+} \right] d\eta \int_{X_-}^{X_+} d\xi + \int_{\eta^-}^{\eta^+} d\eta \left[ \int_{-} + \int_{+} \right] d\xi. \quad (14b)$$

Here affixed symbol  $\pm$  signifies integration over range  $x_+ < \xi < X_+$  and  $X_- < \xi < x_-$ , respectively. Limits  $N^{\pm}(\psi)$  and  $\eta^{\pm}(\psi)$  in (14b) are defined by

$$\Im(\xi_1(\xi, N^{\pm}), \xi_2(\xi, N^{\pm})) = 0, \quad \frac{dN^{\pm}}{d\xi} = 0, \quad (15a)$$

$$f(\xi_1(\xi, \eta^{\pm}), \xi_2(\xi, \eta^{\pm})) = 0, \quad \frac{d\eta^{\pm}}{d\xi} = 0. \quad (15b)$$

That is, for given  $\psi$  limits  $(N^{\pm}, \eta^{\pm})$  are the maximum and minimum values of  $\eta$  on, respectively, the outer and inner contours of  $C$ . For given  $\eta$ , therefore, limits  $X_{\pm}(\psi, \eta)$  and  $x_{\pm}(\psi, \eta)$  locate the ends of lines that run parallel to the  $\xi$ -axis and span the interiors of, respectively, the outer and inner contours of  $C$ . Conditions on  $C$  imply that these limits exist, are single-valued, and vary continuously in  $\psi$ .

### Transform inversion: asymptotic results

Equations (9b), (9c) and (12a) suggest that, in general, a numerical procedure is required for  $p$ -integration in (14a). This is a common situation in coupled thermoelasticity and often, for example, [Wang and Dhaliwal 1993; Brock 2009], an asymptotic inversion is used to produce an analytic result. Calculations [Brock and Georgiadis 2000; Ignaczak and Ostoja-Starzewski 2010] indicate that, typically,

$$h \approx O(10^{-9}) \text{ m}, \quad t_0 \approx O(10^{-13}) \text{ s}, \quad V_S \approx O(10^3) \text{ m/s}, \quad 0.1 < h_0/h < 1.0.$$

Therefore, use of expansions for (8) and (9) in (14a) that are valid for  $|hp| \gg 1$  give results that are especially relevant [Brock 2009] to the study of thermal relaxation effects. In light of (12), (9) gives,

respectively, the exact result and first-order expansion

$$B \rightarrow B\sqrt{p}\sqrt{-p}, \quad B = \sqrt{1 - c^2 \cos^2 \psi}, \quad (16a)$$

$$A_{\pm} \rightarrow A_{\pm}\sqrt{p}\sqrt{-p} + O(1/hp), \quad A_{\pm} = \sqrt{1 - \frac{c^2}{c_{\pm}^2} \cos^2 \psi}. \quad (16b)$$

Boundedness for  $x_3 > 0$  now requires that  $(c, \psi)$  give nonnegative arguments for radical  $(B, A_{\pm})$ , branch cuts  $\text{Re}(p) < 0, \text{Im}(p) = 0$  and  $\text{Re}(p) > 0, \text{Im}(p) = 0$  be introduced for  $\sqrt{\pm p}$ , respectively, and  $\text{Re}(\sqrt{\pm p}) \geq 0$  in the corresponding cut  $p$ -plane. In view of (12) and (16), the linear combination of products  $K_{\Sigma}(p, \psi)\Sigma(\xi, \eta)$  in (14a) for displacement  $u_k$  when  $x_3 = 0$  is

$$u_1: \frac{B}{pR_A} \cos \psi \left[ \frac{2\alpha_V}{h_B p \omega} (A_- - A_+) \theta_C - N \frac{\sigma}{\mu} \right] + \frac{1}{p\omega R_A} \left( N_1 \frac{\tau_1}{\mu} + N_{12} \frac{\tau_2}{\mu} \right), \quad (17a)$$

$$u_2: \frac{B}{pR_A} \sin \psi \left[ \frac{2\alpha_V}{h_B p \omega} (A_- - A_+) \theta_C - N \frac{\sigma}{\mu} \right] + \frac{1}{p\omega R_A} \left( N_2 \frac{\tau_2}{\mu} + N_{12} \frac{\tau_1}{\mu} \right), \quad (17b)$$

$$u_3: \frac{K\alpha_V}{h_B p^2 R_A} (A_- - A_+) \theta_C + \frac{N_3}{p\omega R_A} \frac{\sigma}{\mu} + \frac{N}{pR_A} \left( \cos \psi \frac{\tau_1}{\mu} + \sin \psi \frac{\tau_2}{\mu} \right). \quad (17c)$$

In (17)  $\tau_k = \tau_k(\xi, \eta), \sigma = \sigma(\xi, \eta), \theta_C = \theta_C(\xi, \eta)$  and

$$\omega = \frac{\sqrt{-p}}{\sqrt{p}}. \quad (18)$$

Other terms in (17) are independent of  $p$ :

$$R_A = K_+ A_+ R_- - K_- A_- R_+, \quad (19a)$$

$$N = K_+ A_+ N_- - K_- A_- N_+, \quad (19b)$$

$$N_1 = -R_A + M \cos^2 \psi, \quad N_2 = -R_A + M \sin^2 \psi, \quad N_{12} = M \sin \psi \cos \psi, \quad (19c)$$

$$M = K_+ A_+ M_- - K_- A_- M_+, \quad N_3 = (K_+ - K_-) A_+ A_- c^2 \cos^2 \psi. \quad (19d)$$

Terms in (19) with  $\pm$  subscript are given by

$$R_{\pm} = 4A_{\pm} B - K^2, \quad N_{\pm} = 2A_{\pm} B + K, \quad M_{\pm} = 4A_{\pm} B + K - B^2, \quad (20a)$$

$$K = c^2 \cos^2 \psi - 2, \quad K_{\pm} = 1 - \frac{c_D^2}{c_{\pm}^2}. \quad (20b)$$

Equation (17) shows that  $K_{\Sigma}$ -terms in (14a) have the forms  $(1/p, 1/p^2, 1/p\omega)$ . The respective  $p$ -integration in (14a) gives [Brock 2012a; 2012b]

$$-i\delta(x - \xi), \quad -iH(x - \xi), \quad \frac{1}{i\pi(x - \xi)}. \quad (21)$$

Here  $(\delta, H)$  is the Dirac and step function. Displacement  $u_3$  for  $x_3 = 0$  is of particular interest, and an expression is given in an explicit form in Appendix A.

Component  $R_{\pm}$  of  $R_A$  in (20a) resembles in form the isothermal Rayleigh function [Achenbach 1973]. Indeed, for  $\psi = 0$   $R_A$  exhibits roots  $c = 0$  and  $c = \pm c_A$ , where  $0 < c_A < 1$ , and is positive for  $0 < |c| < c_A$ ,



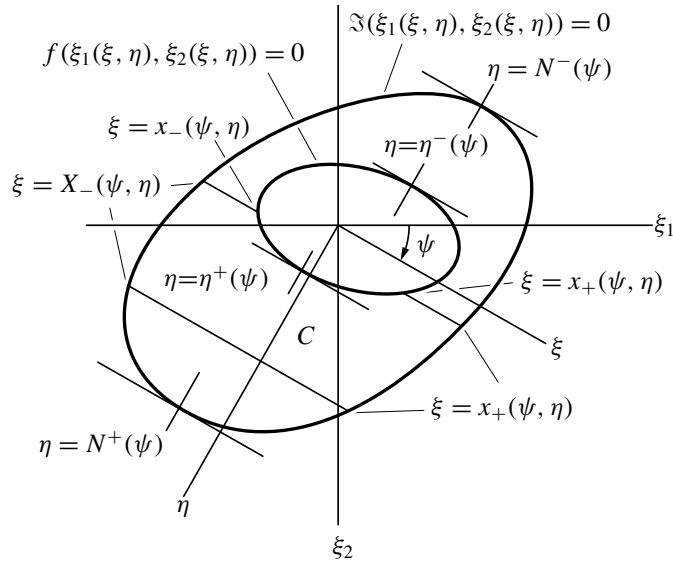


**Figure 2.** Schematic of translating area on surface.

and thus is also a Rayleigh function. Radicals ( $A_{\pm}, B$ ) have nonnegative arguments for  $0 < c \cos \psi < 1$ ,  $|\psi| \leq \pi/2$  and, as noted in connection to (4),  $1 < c_D < c_- < c_+$ . Therefore  $V = c_A V_S < V_S < c_{\pm} V_S$  is the critical speed for translation of area  $C$ . The results of this section are now applied to a study of sliding contact with friction.

### Sliding contact

Consider the half-space treated above, and a rigid die that is a body of revolution with a W-like profile, i.e., it is cup-shaped. Surface temperature of the die is maintained at  $T_C = T_0 + \Theta_C \cos \psi$ , where  $\Theta_C$  is constant. Constant compressive force  $F_3$  is applied to the die and, resisted by sliding friction, the die translates at constant subcritical speed  $V$  in the positive  $x_1$ -direction. A dynamic steady state is assumed, and the process also satisfies (5a) and (5b). However (5c) is modified: For  $x_3 = 0$ ,  $(x_1, x_2) \in C$ ,  $(\tau_1, \tau_2)$  now represent frictional resistance and so are defined by

$$\tau_1 = \gamma \sigma, \quad \tau_2 = 0. \tag{22}$$

Here  $\gamma$  is the coefficient of sliding friction, and normal traction  $\sigma$  is now an unknown, the last condition in (5c) being replaced by

$$u_3 = u_3^0 = U_0 - X_3(x_1, x_2), \tag{23a}$$

$$X_3(x_1, x_2) = \frac{1}{2r_0}(x_1^2 + x_2^2) \left[ 1 - \frac{1}{2r_0^2}(x_1^2 + x_2^2) \right] - \frac{r_0}{4}. \tag{23b}$$

Here  $u_3^0$  is the indentation imposed by the die, with  $U_0$  being the rigid body displacement of the die. Polynomial  $X_3(x_1, x_2)$  gives the die its W-like cross-section, where  $r_0$  is the radial distance between the die axis of symmetry and the “feet” of the W. Results obtained above apply under several conditions: First, area  $C$  includes the initial ( $U_0 = 0$ ) contact contour  $\sqrt{x_1^2 + x_2^2} = r_0$ . Then  $C$  has a ring thickness

that, in light of the fourth-order nature of  $X_3(x_1, x_2)$ , is much smaller than  $r_0$ . Finally,  $\sigma$  must be such that (A1) and (22) give the displacement in (23a). In view of [Brock 2012a; 2012b]

$$u_3^0 = -\frac{1}{\pi} \int_{\Psi} d\psi \iint_C d\eta d\xi \frac{d\delta}{dx}(x - \xi) u_3^0(x_1(\xi, \eta), x_2(\xi, \eta)). \tag{24}$$

So,  $\sigma$  is obtained by matching the integrands of  $(\psi, \eta)$ -integration. In  $\sigma(\xi, \eta)$   $\xi$  is an integration variable representing parameter  $x$  that itself depends on  $(x_1, x_2)$  and integration variable  $\psi$ . As noted in view of (13) for  $y = 0$  however, coordinates  $(x_1, x_2)$  can be replaced by  $(x, \psi)$ . Thus, every point  $(x_1, x_2) \in C$  lies on an integration path  $\eta = 0$  that passes through all four limit points of the  $\xi$ -integral. Thus (A1) and (22)–(25) give for  $x_+ < x < X_+$  and  $X_- < x < x_-$ , respectively, singular integral equation

$$-\frac{N_3}{\mu R_A \pi} \left[ \int_{-}^{+} + (vp) \int_{+} \right] \frac{\sigma(\xi, \psi)}{\xi - x} d\xi + \frac{\gamma N}{R_A} \sigma(x, \psi) \cos \psi = \frac{x}{r_0} \left( 1 - \frac{x^2}{r_0^2} \right) - \frac{T}{r_0} (X_+ - x), \tag{25a}$$

$$-\frac{N_3}{\mu R_A \pi} \left[ (vp) \int_{-} + \int_{+} \right] \frac{\sigma(\sigma, \psi)}{\xi - x} d\xi + \frac{\gamma N}{R_A} \sigma(x, \psi) \cos \psi = \frac{x}{r_0} \left( 1 - \frac{x^2}{r_0^2} \right) - \frac{T}{r_0} (x_- - x), \tag{25b}$$

$$T = -\frac{r_0 K \alpha_V}{h_B R_A} (A_+ - A_-) \Theta_C \cos \psi. \tag{25c}$$

In (25) affixed symbol  $\pm$  signifies integration over, respectively,  $x_+ < \xi < X_+$  and  $X_- < \xi < x_-$ , where  $x_{\pm} = x_{\pm}(\psi)$  and  $X_{\pm} = X_{\pm}(\psi)$ , and  $(vp)$  signifies Cauchy principal value integration. Equation (25) is a classic type [Erdogan 1978], with inhomogeneous terms of polynomial form. The solution is a linear combination of terms

$$x^N \cos \pi \Omega + \frac{\sin \pi \Omega}{\pi} \left( \frac{x - x_-}{x - X_-} \right)^{\Omega} \left( \frac{X_+ - x}{x - x_+} \right)^{\Omega} I_+(x^N) \quad (x_+ < x < X_+), \tag{26a}$$

$$x^N \cos \pi \Omega + \frac{\sin \pi \Omega}{\pi} \left( \frac{X_+ - x}{x_+ - x} \right)^{\Omega} \left( \frac{x_- - x}{x - X_-} \right)^{\Omega} I_-(x^N) \quad (X_- < x < x_-). \tag{26b}$$

In (26)  $N = 0, 1, 3$  and

$$I_+(x^N) = \int_{-} \frac{t^N dt}{t - x} \left( \frac{x_+ - t}{X_+ - t} \right)^{\Omega} \left( \frac{t - X_-}{x_- - t} \right)^{\Omega} + (vp) \int_{+} \frac{t^N dt}{t - x} \left( \frac{t - X_-}{t - x_-} \right)^{\Omega} \left( \frac{t - x_+}{X_+ - t} \right)^{\Omega}, \tag{27a}$$

$$I_-(x^N) = (vp) \int_{-} \frac{t^N dt}{t - x} \left( \frac{x_+ - t}{X_+ - t} \right)^{\Omega} \left( \frac{t - X_-}{x_- - t} \right)^{\Omega} + \int_{+} \frac{t^N dt}{t - x} \left( \frac{t - X_-}{t - x_-} \right)^{\Omega} \left( \frac{t - x_+}{X_+ - t} \right)^{\Omega}, \tag{27b}$$

$$\Omega = -\frac{1}{2} + \frac{1}{\pi} \tan^{-1} \left( -\frac{\gamma N}{N_3} \cos \psi \right). \tag{27c}$$

For sliding contact at subcritical speed (see discussion above) it can be shown that  $N \leq 0$  and  $N_3 \geq 0$ , so that dimensionless exponent satisfies  $-\frac{1}{2} < \Omega < 0$ . Integration formulas (B1)–(B3) in Appendix B lead to, for  $x_+ < x < X_+$  and  $X_- < x < x_-$ , respectively, contact zone normal traction in analytic

form:

$$\frac{\sigma_+}{\mu} = -\frac{R_A}{r_0 S} \left( \frac{x - x_-}{x - X_-} \right)^\Omega \left( \frac{X_+ - x}{x - x_+} \right)^\Omega \left[ (1 + T)G_1(x) - TX_+ - \frac{G_3(x)}{r_0^2} \right], \tag{28a}$$

$$\frac{\sigma_-}{\mu} = -\frac{R_A}{r_0 S} \left( \frac{X_+ - x}{x_+ - x} \right)^\Omega \left( \frac{x - x}{x - X_-} \right)^\Omega \left[ (1 + T)G_1(x) - Tx_- - \frac{G_3(x)}{r_0^2} \right], \tag{28b}$$

$$S = \sqrt{(\gamma N \cos \psi)^2 + N_3^2}. \tag{28c}$$

Equation (28) involves contact zone parameters  $(X_\pm, x_\pm)$ . These can be determined by satisfying auxiliary conditions that must be imposed on the solution.

**Auxiliary conditions**

Because the die is not flat-bottomed, contact zone traction should be continuous at the zone boundaries:

$$\sigma_\pm(X_\pm, \psi) = \sigma_\pm(x_\pm, \psi) = 0. \tag{29a}$$

Continuity of the contact zone contour functions  $(\mathfrak{S}, f)$  requires that

$$X_+(\pi/2) + X_-(-\pi/2) = 0, \quad x_+(\pi/2) + x_-(-\pi/2) = 0. \tag{29b}$$

In light of (C1), (C2), (C3a) and (C4) in Appendix C, imposing (29) on (28) gives

$$\frac{\sigma_+}{\mu} = \frac{R_A}{S} \left( \frac{z - z_-}{z - Z_-} \right)^\Omega \left( \frac{Z_+ - z}{z - z_+} \right)^\Omega (Z_+ - z)[T - (Z_+ + z_- + \Omega l)(z - z_-)], \tag{30a}$$

$$\frac{\sigma_-}{\mu} = \frac{R_A}{S} \left( \frac{Z_+ - z}{z_+ - z} \right)^\Omega \left( \frac{z - z}{z - Z_-} \right)^\Omega (z - z)[T - (Z_+ + z_- + \Omega l)(Z_+ - z)]. \tag{30b}$$

In (30) Equations (B3), (C2) and (C5) are used to introduce dimensionless parameters

$$z = \frac{x}{r_0}, \quad Z_\pm = \frac{X_\pm}{r_0}, \quad z_\pm = \frac{x_\pm}{r_0}, \tag{31a}$$

$$l_\pm = L_\pm/r_0 = \frac{1}{2}(l + \bar{l}), \quad l_- = L_-/r_0 = \frac{1}{2}(l - \bar{l}), \tag{31b}$$

$$\bar{l} = 0 \quad (|\psi| = \pi/2). \tag{31c}$$

Here  $L_\pm$  is the thickness of the two contact zone ring segments measured along a line that passes through  $x = 0$  at angle  $|\psi| \leq \pi/2$ . Under the reasonable assumption that the contact zone ring is “thin” ( $l_\pm \ll 1$ ), imposition of (29a) is shown in Appendix C to give the valid approximations

$$Z_+ = 1 + \frac{1}{2}\Omega(Tl - l - \bar{l}), \quad z_+ = 1 + \frac{1}{2}[\Omega Tl - (1 + \Omega)(l + \bar{l})], \tag{32a}$$

$$z_- = -1 + \frac{1}{2}\Omega(Tl - l + \bar{l}), \quad Z_- = -1 + \frac{1}{2}[\Omega Tl - (1 + \Omega)(l - \bar{l})], \tag{32b}$$

$$Z_+ + z_- + \Omega l = \Omega Tl. \tag{32c}$$

The resultant of contact zone traction must be the compressive force  $F_3$  on the die:

$$\iint_C \sigma(x_1, x_2) dx_1 dx_2 = r_0^2 \int_{\psi} d\psi \left[ \int_{-} |z| \sigma_{-}(z, \psi) dz + \int_{+} |z| \sigma_{+}(z, \psi) dz \right] = -F_3. \quad (33)$$

Affixed symbol  $\pm$  now signifies integration over range  $z_+ < z < Z_+$  and  $Z_- < z < z_-$ . Traction  $\sigma_{\pm}(z, \psi)$  should be stationary with respect to  $F_3$  [Brock 2012a; 2012b; 2014b]:

$$\delta\sigma_{\pm} = \frac{\partial\sigma_{\pm}}{\partial z} \delta z + \frac{\partial\sigma_{\pm}}{\partial\psi} \delta\psi = 0. \quad (34)$$

Because  $(\delta z, \delta\psi)$  are arbitrary, (34) requires for  $|\psi| < \pi/2$  that

$$\frac{\partial\sigma_{\pm}}{\partial z}(z, \psi) = 0(z = z_{\pm}^*), \quad \frac{\partial\sigma_{\pm}}{\partial\psi}(z_{\pm}^*, \psi) = 0. \quad (35)$$

The process for obtaining  $z_{\pm}^*$  is outlined in Appendix D. In keeping with (32), valid approximations are sufficient:

$$z_+^* = 1 + \frac{\Omega}{2}(Tl - l - \bar{l}) - \frac{2(1+\Omega) - T}{2+(1-\Omega)T} \frac{l + \bar{l}}{2}, \quad (36a)$$

$$z_-^* = -1 + \frac{\Omega}{2}(Tl - l + \bar{l}) - \frac{2(1+\Omega) - T}{2+(1-\Omega)T} \frac{l - \bar{l}}{2}. \quad (36b)$$

Use of (32) and (36) in (30) give

$$\frac{\sigma_{\pm}^*}{\mu} = \frac{R_A}{2S} \frac{\Omega - 2}{2 + (1 - \Omega)T} \frac{[2(1 + \Omega) - T]^{1+\Omega}}{[-2\Omega + (2 - \Omega)T]^{\Omega}} (l \pm \bar{l}). \quad (37)$$

For sliding without surface bonding, the contact zone cannot be in tension. Moreover, the radicals in (37) must have positive arguments. Thus unilateral constraints are required. Because  $(R_A, S)$  defined in (19a) and (28c) are positive for subcritical sliding, these are

$$-\frac{2}{1-\Omega} < \frac{2\Omega}{2-\Omega} < T < 2(1+\Omega) < 2. \quad (38)$$

In view of (25c), therefore, sliding contact by the die has a dynamic steady state only if the difference in ambient ( $T_0$ ) and die ( $T_C$ ) temperature satisfies (38). Similar phenomena are noted for a flat contact surface [Jang 2000; 2005] and sliding dies of various profiles in the absence of friction [Brock 2014b]. However, contact zones are simply connected, and restrictions apply only if die temperature exceeds the ambient value.

The second condition in (35) requires that  $\sigma_{\pm}^*$  be invariant with respect to  $\psi$ . In view of (19), (20), (25c), (27c), (28c) and (31c), when  $|\psi| = \pi/2$ , we have

$$\Omega = -\frac{1}{2}, \quad T = 0, \quad \bar{l} = 0, \quad \frac{R_A}{S} = \frac{2(c_D^2 - 1)}{\sqrt{c_D^4 + \gamma^2}}. \quad (39)$$

Thus (37) gives two equations for  $(l, \bar{l})$  at any  $|\psi| < \pi/2$  in terms of the unknown  $l$  at  $|\psi| = \pi/2$ . We identify it as  $l_2$ , i.e., a measurement taken along the  $x_2$ -axis, and find that

$$l = \frac{2(c_D^2 - 1)S}{R_A \sqrt{c_D^2 + \gamma^2}} Q l_2, \quad \bar{l} = 0, \quad (40a)$$

$$Q = \frac{2 + (1 - \Omega)T}{2 - T} \frac{[-2\Omega + (2 - \Omega)T]^\Omega}{[2(1 + \Omega) - T]^{1+\Omega}}. \quad (40b)$$

A valid approximation to the  $z$ -integration in (33) involving (30) can, under (again) the expectation that  $(l, \bar{l}) \ll 1$ , be obtained. In view of (40a) this leads to an equation for the unknown  $l_2$ . Introduction of the integration variable  $t = c \cos \psi$  renders this as

$$\frac{F_3}{\mu r_0^2} = \frac{\pi(c_D^2 - 1)^2}{c_D^4 + \gamma^2} l_2^2 \int_0^c \frac{R_A dt}{S \sqrt{c^2 - t^2}} \frac{\Omega(1 + \Omega)}{\sin \pi \Omega} Q^2. \quad (41)$$

With  $l_2$  in hand, the solution process is complete.

### Sample calculations

For insight into restriction (38), die-ambient temperature difference is examined along the translating  $x_1$ -axis, that is,  $\psi = 0$ ,  $T_C - T_0 = \Theta_C$ . Values of parameter  $\Omega$  and the relevant maximum and minimum  $\Theta_C^\pm$  defined by (25c) and (38), for subcritical (dimensionless) translation speed  $c$  and friction coefficient  $\gamma$ , appear in Table 1. The half-space is modeled as a generic thermoelastic solid with properties

$$\begin{aligned} V_S &= 3094 \text{ m/s}, & \mu &= 75 \text{ GPa}, & \alpha_V &= 89.6(10^{-6})\text{K}^{-1}, \\ h &= 2.1862(10^{-10}) \text{ m}, & h_0 &= 2.3206(10^{-9}) \text{ m}, & \epsilon &= 0.05794, \\ c_D &= 2.0, & c_F &= 2.0144, & c_+ &= 3.0856, & c_- &= 2.3151, & c_A &= 0.933. \end{aligned}$$

The effect of die geometry and surface convection is represented by ratio

$$\frac{h_B}{r_0} = 4(10^{-4}).$$

Generic properties used in [Brock 2009; 2012b; 2014b] represent solids with more pronounced thermal relaxation. Thus, the dimensionless speeds  $c_\pm$  are somewhat larger than the values given above. Table 1 shows that die temperatures that lie below the ambient value are the more restricted. For given friction level ( $\gamma$ ), the range of allowable  $\Theta_C$  decreases as die translation speed ( $c$ ) increases. For given translation speed, the range decreases as friction level increases. Equations (25c) and (38) show, however, that the range will increase when convection ratio  $h_B/r_0$  is increased. The ranges indicated by Table 1 entries seems narrow, but the governing equations (1)–(4) themselves are based on the assumption that temperature change in the solid renders a small ratio  $|\theta/T_0|$ .

For insight into contact zone geometry, calculations for ratio  $l/l_2$  are given in Table 2 for the same generic solid. Parameters  $(l, l_2)$  are the widths of the ring formed by the contact zone as measured along lines  $|\psi| \neq 90^\circ$  and  $|\psi| = 90^\circ$ . In view of (40a), the ring of initial contact  $\sqrt{x_1^2 + x_2^2} = r_0$  (approximately) bisects these widths. Formulas such as (38) are based on the assumption that  $(l, l_2)/r_0 \ll 1$ . Thus, Table 2 entries show that the contact zone ring generated by compression and die translation is only approximately

	$c = 0.1$	$c = 0.2$	$c = 0.3$	$c = 0.4$	$c = 0.5$
	$\gamma = 0.1$				
$\Omega$	-0.4920	-0.4918	-0.4915	-0.4911	-0.4905
$\Theta_C^+(\text{°C})$	27.255	26.244	25.715	24.751	23.391
$\Theta_C^-(\text{°C})$	-10.594	-10.193	-9.978	-9.588	-9.041
	$\gamma = 0.2$				
$\Omega$	-0.4841	-0.4837	-0.4831	-0.4822	-0.481
$\Theta_C^+(\text{°C})$	27.682	26.665	26.142	25.184	23.828
$\Theta_C^-(\text{°C})$	-10.456	-10.057	-9.839	-9.449	-8.899
	$\gamma = 0.5$				
$\Omega$	-0.4604	-0.4594	-0.4579	-0.4558	-0.4527
$\Theta_C^+(\text{°C})$	28.954	27.921	27.415	26.468	25.126
$\Theta_C^-(\text{°C})$	-10.04	-9.646	-9.422	-9.027	-8.473

**Table 1.** Parameter  $\Omega$ , maximum (+) and minimum (-)  $\Theta_C$  for  $\chi(c)(\psi = 0)$ .

$l/l_2$	$c = 0.1$	$c = 0.2$	$c = 0.3$	$c = 0.4$	$c = 0.5$
	$\gamma = 0.1$				
$\psi = 0^\circ$	1.4247	1.4882	1.5654	1.6984	1.9199
$\psi = 45^\circ$	1.4366	1.4578	1.4936	1.5490	1.6289
$\psi = 90^\circ$	1.0	1.0	1.0	1.0	1.0
	$\gamma = 0.2$				
$\psi = 0^\circ$	1.4243	1.4885	1.565	1.698	1.9194
$\psi = 45^\circ$	1.4356	1.4567	1.4928	1.5481	1.6278
$\psi = 90^\circ$	1.0	1.0	1.0	1.0	1.0
	$\gamma = 0.5$				
$\psi = 0^\circ$	1.4213	1.4850	1.5625	1.6957	1.9179
$\psi = 45^\circ$	1.4295	1.4506	1.4865	1.5417	1.6275
$\psi = 90^\circ$	1.0	1.0	1.0	1.0	1.0

**Table 2.** Ratio  $l/l_2$  for  $\chi, \psi, c$  when  $\Theta_C = 10^\circ\text{C}$  ( $\Theta_C^- < \Theta_C < \Theta_C^+$ ).

circular. Parameter  $l_2$  is the minimum width, but  $l$  along the travel direction ( $\psi = 0$ ) is not the maximum width. This behavior is consistent with that for the simply connected contact zones considered in [Rahman 1996] and [Brock 2012a; 2012b; 2014b]. That is, the contact zone does not replicate the projection of the die profile onto the surface, and friction and direction and speed of translation are factors. Table 2 data indicate that here the friction effect is not as noticeable as that for translation speed and direction.

### Summary comments

This 3D, thermoelastic study indicates that a simply connected and a ring-like contact zone created by a sliding die share some characteristics: Die sliding speed and temperature, thermal relaxation and convection, and friction influence zone shape. The projection of die profile onto the surface may not adequately describe zone shape. In two respects, they may differ: For the simply connected zone, a dynamic steady state will not occur if die temperature exceeds ambient temperature by a critical value. For the ring-like zone, a critical value also exists for a die temperature that lies below ambient temperature. The influence of friction is less pronounced for the ring-like zone.

A cup-shaped die implies the ring-like contact zone, and an asymptotic transform inversion process renders solutions in analytic form. The assumption that contact zone size is “small” is manifest here in terms of ring width, and is used to justify robust, but approximate, expressions for contact zone geometry parameters. In [Brock 2012b] the asymptotic inversion process highlights solution behavior associated with the Fourier model [Boley and Weiner 1985]. Here and in [Brock 2014b], the process highlights behavior associated with the Lord and Shulman [1967] thermal relaxation model. In general, (see [Boley and Weiner 1985; Wang and Dhaliwal 1993], for example), and corresponds to the inversion process for the long-time transient solution. The latter is less so, and inversion corresponds to that for the short-time transient solution.

This work is part of a dynamic steady state study of 3D contact problems on isothermal and thermoelastic half-spaces. Anisotropy is also included, for example, [Brock 2014a]. The dynamic steady state is simpler to analyze than the transient, and is often sufficient to model sliding contact processes [Bayer 1994; Blau 1996].

The study makes use of exact expressions for multiple integral transforms associated with a related unmixed boundary value problem. The basis is Cartesian, but the inversion process — whether exact or asymptotic — introduces quasipolar coordinates. This hybridization produces expressions that lead readily to the formulation of the mixed 3D contact problem in terms of classical singular integral equations [Erdogan 1978]. Axial symmetry is not required.

The study — including this work — does involve contact zones for which the singular integral equations hold over the span of the zone, in whatever direction that span is taken. Inflections in contact zone contour, or multiple “holes” in the zone, create equation forms that are span-dependent. However, this complication need not preclude use of the basic approach.

### Appendix A

An expression for displacement  $u_3$  when  $x_3 = 0$  can be obtained from (12b), (14a), (17c) and (21) in an explicit form:

$$\begin{aligned}
 u_3 = & -\frac{1}{\pi} \int_{\Psi} \frac{N_3}{\mu\pi R_A} d\psi \times \left[ \int_{N^-}^{\eta^-} + \int_{\eta^+}^{N^+} \right] d\eta \int_{X_-}^{X_+} \frac{\sigma(\xi, \eta)}{\xi - x} d\xi + \int_{\eta^-}^{\eta^+} d\eta \left[ \int_{-} + \int_{+} \right] \frac{\sigma(\xi, \eta)}{\xi - x} d\xi \\
 & + \frac{\alpha_V}{h_B} \int_{\Psi} \frac{K}{\pi R_A} (A_- - A_+) d\psi \times \left[ \int_{\eta^-} + \int_{\eta^+} \right] d\eta \int_{X_-}^x \theta_C(\xi, \eta) d\xi H(X_+ - x) \\
 & + \int_{\eta^-}^{\eta^+} d\eta \left[ \int_{-} H(x_- - x) + \int_{+} H(X_+ - x) \right] \theta_C(\xi, \eta) d\xi + (continued)
 \end{aligned}$$



$$\begin{aligned}
& + \int_{\Psi} \frac{N \cos \psi}{\mu \pi R_A} d\psi \times \left[ \int_{N^-}^{\eta^-} + \int_{\eta^+}^{N^+} \right] d\eta \int_{-} \tau_1(\xi, \eta) \delta(\xi - x) d\xi \\
& + \int_{\eta^-}^{\eta^+} d\eta \left[ \int_{-} + \int_{+} \right] \tau_1(\xi, \eta) \delta(\xi - x) d\xi \\
& + \int_{\Psi} \frac{N \sin \psi}{\mu \pi R_A} d\psi \times \left[ \int_{N^-}^{\eta^-} + \int_{\eta^+}^{N^+} \right] d\eta \int_{-} \tau_2(\xi, \eta) \delta(\xi - x) d\xi \\
& + \int_{\eta^-}^{\eta^+} d\eta \left[ \int_{-} + \int_{+} \right] \tau_2(\xi, \eta) \delta(\xi - x) d\xi. \tag{A1}
\end{aligned}$$

Here affixed symbol  $\pm$  indicates that integration is over the range  $x_+ < \xi < X_+$  and  $X_- < \xi < x_-$ . For  $(x_1, x_2) \in C$  Cauchy principal value integration (*vp*) is necessary when  $x$  lies the range of  $\xi$ -integration for  $\sigma$ . In corresponding fashion  $\xi$ -integration of  $(\tau_1, \tau_2)$  is replaced with  $\tau_1(x, \eta)$  and  $\tau_2(x, \eta)$ , respectively.

### Appendix B

Application of Cauchy theory to integrals (26a) and (26b) leads to the result

$$\begin{aligned}
G_N(x) &= x^N \left( \frac{x - X_-}{x - x_-} \right)^\Omega \left( \frac{x - x_+}{X_+ - x} \right)^\Omega \cos \pi \Omega + \frac{\sin \pi \Omega}{\pi} I_+(x^N) \\
G_N(x) &= x^N \left( \frac{x_+ - x}{X_+ - x} \right)^\Omega \left( \frac{x - X_-}{x_- - x} \right)^\Omega \cos \pi \Omega + \frac{\sin \pi \Omega}{\pi} I_-(x^N). \tag{B1}
\end{aligned}$$

In (B1) we have

$$G_0(x) = 1, \tag{B2a}$$

$$G_1(x) = xG_0(x) + \Omega L, \tag{B2b}$$

$$G_2(x) = xG_1(x) + \frac{1}{2}\Omega(\Omega L^2 - L_+^2 - L_-^2) + \Omega(X_+L_+ + x_-L_-), \tag{B2c}$$

$$G_3(x) = xG_2(x) + \Omega[X_+L_+(X_+ + \Omega L - L_+) + x_-L_-(x_- + \Omega L - L_-)] + \frac{1}{6}\Omega(1 - \Omega)(2 - \Omega)L^3. \tag{B2d}$$

In (B2) the lengths are

$$L = L_+ + L_-, \quad L_+ = X_+ - x_+, \quad L_- = x_- - X_-. \tag{B3}$$

Terms  $L_\pm$  give the thickness of the two sides of the contact zone ring measured along the line passing through  $x = 0$  at a given angle  $-\pi/2 < \psi < \pi/2$ .

### Appendix C

Because  $\Omega < 0$ , (28) shows that (29a) is satisfied only if

$$X_+ + (1 + T)L - \frac{G_3(X_+)}{r_0^2} = 0, \quad x_- + (1 + T)L - \frac{G_3(x_-)}{r_0^2} = 0. \tag{C1}$$

At this point it is convenient to introduce dimensionless parameters

$$z = \frac{x}{r_0}, \quad Z_{\pm} = \frac{X_{\pm}}{r_0}, \quad z_{\pm} = \frac{x_{\pm}}{r_0}, \quad l = \frac{L}{r_0}, \quad l_{\pm} = \frac{L_{\pm}}{r_0}. \quad (\text{C2})$$

In light of (B2) and (B3), (C1) can be written as

$$Z_+ + (1 + T)l - \bar{G}_3(Z_+) = 0, \quad z_- + (1 + T)l - \bar{G}_3(z_-) = 0, \quad (\text{C3a})$$

$$\bar{G}_1(z) = z + \Omega l, \quad (\text{C3b})$$

$$\bar{G}_2(z) = z\bar{G}_1(z) + \frac{1}{2}\Omega(\Omega l^2 - l_+^2 - l_-^2) + \Omega(Z_+l_+ + z_-l_-), \quad (\text{C3c})$$

$$\bar{G}_3(z) = z\bar{G}_2(z) + \Omega[Z_+l_+(Z_+ + \Omega l - l_+) + z_-l_-(z_- + \Omega l - l_-)] + \frac{1}{6}\Omega(1 - \Omega)(2 - \Omega)l^3. \quad (\text{C3d})$$

Either of the equations in (C3a) can be replaced by the difference in the two:

$$Z_+^2 + z_-^2 + Z_+z_- + \Omega l \left( Z_+ + z_- + \frac{\Omega l}{2} \right) + \Omega \left[ l_+ \left( Z_+ - \frac{l_+}{2} \right) + l_- \left( z_- - \frac{l_-}{2} \right) \right] - 1 = 0. \quad (\text{C4})$$

Equation (C3a) are coupled equations for  $(Z_+, z_-)$  in terms of (dimensionless) contact zone ring thickness  $(l, l_{\pm})$ . Parameters  $(z_+, Z_-)$  then follow as

$$z_+ = Z_+ - l_+, \quad Z_- = z_- - l_-. \quad (\text{C5})$$

Because (C4) is quadratic, it is not difficult to rewrite (C3a) as uncoupled sixth-order equations for  $Z_+$  and  $z_-$ . For small deformation, however, (23b) implies that the ring is “thin”, with mean radius  $r_0$ . That is,  $l_{\pm} \ll 1$  and we assume that  $Z_+ \approx 1 + P_+(l_{\pm}) + O(l_{\pm}^2, l_+l_-)$  and  $z_- \approx -1 + P_-(l_{\pm}) + O(l_{\pm}^2, l_+l_-)$ . It can then be shown that (C3a) and (C5) give

$$Z_+ \approx 1 + \Omega \left( \frac{T}{2}l - l_+ \right), \quad z_- \approx -1 + \Omega \left( \frac{T}{2}l - l_- \right). \quad (\text{C6})$$

Parameters  $(l, l_{\pm})$  are not independent, so it is convenient to use  $(l, \bar{l})$ , where

$$l = l_+ + l_-, \quad \bar{l} = l_+ - l_-. \quad (\text{C7})$$

Then (C5) and (C6) give

$$l_{\pm} = \frac{1}{2}(l \pm \bar{l}), \quad (\text{C8a})$$

$$Z_+ \approx 1 + \frac{1}{2}\Omega(Tl - l - \bar{l}), \quad z_+ \approx 1 + \frac{1}{2}[\Omega Tl - (1 + \Omega)(l + \bar{l})], \quad (\text{C8b})$$

$$z_- \approx -1 + \frac{1}{2}\Omega(Tl - l + \bar{l}), \quad Z_- \approx -1 + \frac{1}{2}[\Omega Tl - (1 + \Omega)(l - \bar{l})]. \quad (\text{C8c})$$

In view of (25c) and (27c), Equation (C8) indicates that condition (29b) is satisfied when

$$\bar{l} = 0 \quad (|\psi| = \pi/2). \quad (\text{C9})$$

## Appendix D

Use of (28a) in the first equation in (35) gives the fifth-order equation for  $z_+^*$ :

$$\begin{aligned}
& (z_+^* - z_+)(Z_+ - z_+^*)(z_+^* - Z_-)(z_+^* - z_-)^2 \\
& \quad + (z_+^* + \Omega T l)(z_+^* - z_-)(Z_+ - z_+^*)(z_+^* - z_+)[z_+^* + \Omega z_- - (1 + \Omega)Z_-] \\
& \quad - (z_+^* - z_-)(z_+^* - Z_-)[z_+^* + \Omega Z_+ - (1 + \Omega)z_+] \\
& \quad + T[\Omega(z_+ - Z_+)(z_+^* - z_-)(z_+^* - Z_-) + \Omega(Z_+ - z_-)(z_+^* - z_+)(z_+^* - Z_-)] \\
& \quad + T[\Omega(z_- - Z_-)(z_+^* - z_+)(z_+^* - z_-) - (z_+^* - z_+)(z_+^* - z_-)(z_+^* - Z_-)] = 0. \quad (D1)
\end{aligned}$$

In the expectation that  $(l, \bar{l}) \ll 1$ , approximations (C8) and  $z_+^* \approx 1 + P^*(l, \bar{l})$  are employed in (D1), with result

$$z_+^* \approx 1 + \frac{\Omega}{2}(Tl - l - \bar{l}) - \frac{2(1 + \Omega) - T}{2 + (1 - \Omega)T} \frac{l - \bar{l}}{2}. \quad (D2a)$$

In similar fashion use of (28b) in (35) gives

$$z_-^* \approx -1 + \frac{\Omega}{2}(Tl - l + \bar{l}) - \frac{2(1 + \Omega) - T}{2 + (1 - \Omega)T} \frac{l - \bar{l}}{2}. \quad (D2b)$$

## References

- [Achenbach 1973] J. D. Achenbach, *Wave propagation in elastic solids*, North-Holland Series in Applied Mathematics and Mechanics **16**, Elsevier, Amsterdam, 1973.
- [Ahmadi et al. 1983] N. Ahmadi, L. M. Keer, and T. Mura, “Non-Hertzian contact stress analysis for an elastic half space: normal and sliding contact”, *Int. J. Solids Struct.* **19**:4 (1983), 357–373.
- [Barber 1992] J. R. Barber, *Elasticity*, Solid Mechanics and its Applications **12**, Kluwer, Dordrecht, 1992.
- [Bayer 1994] R. G. Bayer, *Mechanical wear prediction and prevention*, Mechanical Engineering **91**, Dekker, New York, 1994.
- [Blau 1996] P. J. Blau, *Friction science and technology*, Dekker, New York, 1996.
- [Boley and Weiner 1985] B. A. Boley and J. H. Weiner, *Theory of thermal stresses*, Krieger, Malabar, FL, 1985.
- [Brock 2009] L. M. Brock, “Basic problems of coupled thermoelasticity with thermal relaxation and pre-stress: aspects observed in exact and asymptotic solutions”, *J. Therm. Stresses* **32**:6-7 (2009), 593–622.
- [Brock 2012a] L. M. Brock, “Two cases of rapid contact on an elastic half-space: sliding ellipsoidal die, rolling sphere”, *J. Mech. Mater. Struct.* **7**:5 (2012), 469–483.
- [Brock 2012b] L. M. Brock, “Two cases of rapid contact on a coupled thermoelastic half-space: sliding ellipsoidal die, rolling sphere”, *J. Therm. Stresses* **35**:11 (2012), 1018–1036.
- [Brock 2014a] L. M. Brock, “Rapid sliding contact in three dimensional (*sic*) by an ellipsoidal die on transversely isotropic half-spaces with surfaces on different principal planes”, *J. Appl. Mech. (ASME)* **81**:3 (2014), Art. ID #031005.
- [Brock 2014b] L. M. Brock, “The rigid die on a half-space with thermal relaxation and convection: influence of sliding speed, die temperature, and geometry”, *J. Therm. Stresses* **37**:7 (2014), 832–851.
- [Brock and Georgiadis 2000] L. M. Brock and H. G. Georgiadis, “Sliding contact with friction of a thermoelastic solid at subsonic, transonic, and supersonic speeds”, *J. Therm. Stresses* **23**:7 (2000), 629–656.
- [Churilov 1978] V. A. Churilov, “Action of an elliptic stamp moving at a constant speed on an elastic half-space”, *Prikl. Mat. Mekh.* **42**:6 (1978), 1074–1079. In Russian; translated in *J. Appl. Math. Mech.* **42**:6 (1978), 1176–1182.
- [Craggs and Roberts 1967] J. W. Craggs and A. M. Roberts, “On the motion of a heavy cylinder over the surface of an elastic solid”, *J. Appl. Mech. (ASME)* **34**:1 (1967), 207–209.
- [Erdogan 1978] F. Erdogan, “Mixed boundary value problems in mechanics”, pp. 1–86 in *Mechanics today*, vol. 4, edited by S. Nemat-Nasser, Pergamon, New York, 1978.

- [Ignaczak and Ostoja-Starzewski 2010] J. Ignaczak and M. Ostoja-Starzewski, *Thermoelasticity with finite wave speeds*, Oxford University Press, 2010.
- [Jang 2000] Y.-H. Jang, “Transient thermoelastic contact problems for an elastic foundation”, *Int. J. Solids Struct.* **37**:14 (2000), 1997–2004.
- [Jang 2005] Y.-H. Jang, “Effects of thermal contact resistance on transient thermoelastic contacts for an elastic foundation”, *J. Appl. Mech. (ASME)* **72**:6 (2005), 972–977.
- [Lord and Shulman 1967] H. W. Lord and Y. Shulman, “A generalized dynamical theory of thermoelasticity”, *J. Mech. Phys. Solids* **15**:5 (1967), 299–309.
- [Rahman 1996] M. Rahman, “Hertz problem for a rigid punch moving across the surface of a semi-infinite elastic solid”, *Z. Angew. Math. Phys.* **47**:4 (1996), 601–615.
- [Sneddon 1972] I. N. Sneddon, *The use of integral transforms*, McGraw-Hill, New York, 1972.
- [Wang and Dhaliwal 1993] J. Wang and R. S. Dhaliwal, “Fundamental solutions of the generalized thermoelastic equations”, *J. Therm. Stresses* **16**:2 (1993), 135–161.

Received 15 Apr 2014. Accepted 7 Jul 2014.

LOUIS MILTON BROCK: [louis.brock@uky.edu](mailto:louis.brock@uky.edu)

*Department of Mechanical Engineering, University of Kentucky, 265 RGAN, Lexington, KY 40506-0503, United States*



# JOURNAL OF MECHANICS OF MATERIALS AND STRUCTURES

[msp.org/jomms](http://msp.org/jomms)

Founded by Charles R. Steele and Marie-Louise Steele

## EDITORIAL BOARD

ADAIR R. AGUIAR	University of São Paulo at São Carlos, Brazil
KATIA BERTOLDI	Harvard University, USA
DAVIDE BIGONI	University of Trento, Italy
IWONA JASIUK	University of Illinois at Urbana-Champaign, USA
THOMAS J. PENCE	Michigan State University, USA
YASUhide SHINDO	Tohoku University, Japan
DAVID STEIGMANN	University of California at Berkeley

## ADVISORY BOARD

J. P. CARTER	University of Sydney, Australia
D. H. HODGES	Georgia Institute of Technology, USA
J. HUTCHINSON	Harvard University, USA
D. PAMPLONA	Universidade Católica do Rio de Janeiro, Brazil
M. B. RUBIN	Technion, Haifa, Israel

**PRODUCTION** [production@msp.org](mailto:production@msp.org)

SILVIO LEVY Scientific Editor

---

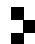
See [msp.org/jomms](http://msp.org/jomms) for submission guidelines.

JoMMS (ISSN 1559-3959) at Mathematical Sciences Publishers, 798 Evans Hall #6840, c/o University of California, Berkeley, CA 94720-3840, is published in 10 issues a year. The subscription price for 2014 is US\$555/year for the electronic version, and \$710/year (+\$60, if shipping outside the US) for print and electronic. Subscriptions, requests for back issues, and changes of address should be sent to MSP.

---

JoMMS peer-review and production is managed by EditFLOW<sup>®</sup> from Mathematical Sciences Publishers.

PUBLISHED BY

 **mathematical sciences publishers**  
nonprofit scientific publishing

<http://msp.org/>

© 2014 Mathematical Sciences Publishers

# Journal of Mechanics of Materials and Structures

Volume 9, No. 3

May 2014

---

- B-splines collocation eigenanalysis of 2D acoustic problems**  
CHRISTOPHER G. PROVATIDIS 259
- Multi-region Trefftz collocation grains (MTCGs) for modeling piezoelectric composite and porous materials in direct and inverse problems**  
PETER L. BISHAY, ABDULLAH ALOTAIBI and SATYA N. ATLURI 287
- Analytical solution for ductile and FRC plates on elastic ground loaded on a small circular area**  
ENRICO RADI and PIETRO DI MAIDA 313
- Solution of a receding contact problem using an analytical method and a finite element method**  
ERDAL ÖNER, MURAT YAYLACI and AHMET BIRINCI 333
- Sliding of a cup-shaped die on a half-space: influence of thermal relaxation, convection and die temperature**  
LOUIS MILTON BROCK 347



1559-3959(2014)9:3;1-7